# ICSO 2016

# International Conference on Space Optics

Biarritz, France

18–21 October 2016

## *Freeform mirror based optical systems for nano-satellites*

*T. Agócs*

*R. Navarro*

*N. Tromp*

*R. Vink*

*et al.*

## FREEFORM MIRROR BASED OPTICAL SYSTEMS FOR NANO-SATELLITES

T. Agócs[1], R. Navarro[1], N. Tromp[1], R. Vink[2]
*[1]NOVA Optical Infrared Instrumentation Group at ASTRON, P.O. Box 2, 7990 AA, The Netherlands;*
*[2]ESA, Keplerlaan 1, 2201 AZ, Noordwijk, The Netherlands;*

INTRODUCTION

High resolution satellite imagery is essential in a wide variety of applications such as urban monitoring, environmental protection, disaster response, precision farming, defence and security. State of the art micro-satellites are able to reach sub-meter ground resolution. These instruments are based on classical two, three or four mirror optical systems and the surfaces are rotationally symmetric or sections of rotationally symmetric surfaces. For nano-satellites, with very limited volume and mass budget, the primary mirror segments are needed to be deployed in order to create the final operational primary configuration that spans over a sufficiently large area. As a result of packaging, mass and space allocation requirements, the primary mirror segments don't deploy into a complete optical aperture, instead sub-apertures are formed with arbitrary (usually rectangular) shapes. Synthetic aperture telescope systems, such as the Michelson or the Fizeau type can be used to achieve sub-meter resolution, the latter being generally more practical due to its relative simplicity. Due to the highly truncated optical apertures (creating non-circular shapes), it is worth to investigate how freeform surfaces (without any rotation symmetry) can be used in these optical architectures. In the current paper we study various freeform mirror based optical system concepts for nano-satellites and investigate what is the performance increase with respect to image quality, field of view and compactness. We present various freeform based systems with significant performance gain. We also investigate convergence during the optimization process and the robustness of the created solutions are further studied. We use freeform optimization techniques to create different freeform based optical architectures that we compare with conventional optical designs. We discuss the necessary manufacturing techniques to create the freeform optical surfaces and detail the metrology to verify the manufacturing and alignment of the complete system. We build our work on the experience that we gained in the OPTICON FP7 Freeform Active Mirror Experiment (FAME) project [1].

I. REQUIREMENTS AND SYSTEM TRADE-OFF

In order to achieve sub-meter resolution on Earth, the following is required from the optical system of the Earth observing satellite. Considering a 300km flying altitude, a target Modulation Transfer Function (MTF) of 0.1 at both the Nyquist frequency as well as half this frequency, the necessary telescope aperture size can be derived. In the ideal case, when the telescope entrance pupil has a circular shape, a 200mm diameter aperture will result a PSF FWHM of 0.8m on ground and <1m resolution (using Rayleigh criterion). In order to reach the target MTF requirement, the Full Width of Half Maximum (FWHM) of the diffraction limited Point Spread Function (PSF) should be slightly under-sampled by 1.4 pixels (sampling wavelength 550nm). It also means that a 0.6m Ground Sampling Distance (GSD) should be delivered by the instrument.

**Table 1** Considered requirements

| Requirement | Specification | Notes |
|---|---|---|
| **HIGH LEVEL REQ. AND DESIGN CONSTRAINTS:** | | |
| **Volume of optical system** | 2U | |
| **Spatial resolution on ground** | <1m | |
| **MTF at Nyquist freq. and half Nyquist freq.** | >0.1 | |
| **Flight altitude** | 300km | |
| **Detector pixel size** | 10µm | |
| **Detector resolution** | 1k x 1k, 2k x 128 | Square detector and TDI detector with 128 stages |
| **Nominal λ** | 550nm | |
| **DERIVED REQUIREMENTS:** | | |
| **Ground Sampling Distance** | 0.6m | PSF is slightly under-sampled to achieve MTF requirement |
| **Image quality** | Diff. limited at nominal λ | Best possible image quality |
| **Focal length** | 5000 mm | |
| **Field of view (FOV)** | 0.11 x 0.11 deg$^2$, 0.22 x 0.014 deg$^2$ | Resulting from detector resolution |
| **Entrance pupil (EP) diameter** | ~200mm | Circular EP that delivers 1m spatial resolution on ground |

The requirements and design constraints considered for this paper are summarized in Table 1. Thinking about CubeSats and choosing 2U maximum volume for the optical system, several options can be considered to achieve ~1m resolution on ground. In the following three scenarios are presented. Entrance pupil shape and size, PSF characteristics and MTF curves are shown for each in Table 2 and Table 3 (for comparison the circular entrance pupil scenario is also shown).

- One solution is to use four primary mirror segments, each having a 100mm x 100mm size, each conveniently covering one side of 1U cube. By deploying the four mirrors, an entrance pupil diameter of ~300mm can be achieved, which corresponds to a ~0.7m spatial resolution on ground. In this case the four mirror segments have to form a single optical surface and so co-phasing of the segments is necessary. This requires a sophisticated metrology and actuator system that significantly increases the complexity of the instrument. Furthermore, the segmented primary mirror results in the MTF of the system being far from ideal and especially at the half Nyquist frequency the contrast is very poor.
- Keeping in mind the 2U maximum volume, one could think of only one deployable mirror, which has a 200mm x 100mm rectangular aperture, the larger side of 2U. The spatial resolution on ground would be met only in one direction, in the perpendicular direction it would be two times larger, approximately 2m. Nevertheless, only one deployable mirror would reduce complexity significantly and by having all the other elements of the optical system fixed and stable with respect to each other inside the 2U volume, a simple, but viable instrument could be created.
- Following the same philosophy and considering only one deployable mirror with the size of 200mm x 100mm, but additionally increasing the entrance pupil by another 200mm x 50mm mirror, a large portion of 200mm x 200mm square area would be covered, which is suitable of achieving the 1m spatial resolution on ground in both directions. In this case the 200mm x 50mm mirror would be fixed inside the 2U volume (not deployable), together with the rest of the optical system. Apart from the possible gain in signal to noise, resolution and MTF, the fixed mirror also offers the possibility to do the verification of the optical system in a more efficient way and even if the deployable mirror is not (or can not be) used, the rest of the system can still deliver satellite imagery but with lower resolution and reduced contrast. Additionally, the primary can be aligned and phased more easily, using the fixed primary telescope segment. The design's PSF is very similar and the MTF is better, when compared to telescope based on four primary segments (lowest two rows in Table 2 and Table 3). Overall, the instrument based on this optical design can be a very good test-bed for numerous purposes, which is ideal for a CubeSat.

Due to the low Earth orbit and high spatial resolution, a very fast detector is needed, which is capable of taking exposures in just several tenth of µs, while the satellite passes over one pixel on ground. It means that a Time Delay and Integration (TDI) detector is needed and 5-10 µm pixel size is considered as a common value for such detectors, 10 µm pixel size being more realistic for lower detector resolutions (we aim at 1k-2k). TDI detectors are strongly elongated rectangular in shape, across track direction resolution ranges from 1k to 12k, while along track direction there are 32-256 stages (lines). As a requirement for our optical designs we investigate two detector configurations: (1) square area that corresponds to 1k x 1k detector with 10 µm pixel size and (2) a rectangular area that corresponds to a 2k x 128 pixel TDI detector with the same 10 µm pixel size. In this way we can have an idea on the field dependence of the optical properties of the specific optical designs and we also keep open the possibility of detectors with different formats that can satisfy requirements of different applications.

The focal ratios of the three scenarios presented are around F25, which means that very long focal length is needed for a very small volume, which is extremely challenging, but well suited for a system that is based on freeform optical surfaces. In the present paper we will focus on the optical designs that are based on rectangular apertures (designs shown in Table 3), since moving away from circular apertures also offers the opportunity to benefit from freeform surfaces, especially if the rectangular shape coincides with the area of orthogonality of the polynomials that represent the freeform surface. There are other advantages of freeform surfaces in optical designs as well. With the use of freeform surfaces, very compact designs with a smaller space envelope and lower mass can be achieved. In many cases the number of optical surfaces can be reduced, thus throughput can be increased. The geometric aberrations can be reduced, better balanced and controlled, optical performance (image quality, depth of field, field of view, etc.) can be improved. When the rotational symmetry is broken, e.g. the system has eccentric pupil or used off-axis, freeforms outperform rotationally symmetric optical surfaces. Another advantage is that tailor made optimizations can be done, e.g. the overall space envelope can be elongated in one direction, while it can stay narrow in the other or tilted/decentered components can be used and the introduced aberrations can be balanced.

**Table 2** Circular and 4 square segments based entrance pupils and their PSF-s. The deployable segments are shown in green, the fixed ones in blue.
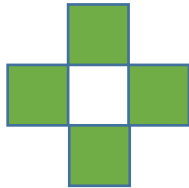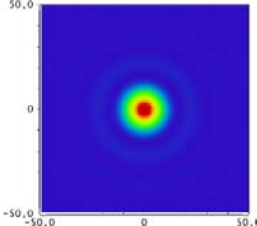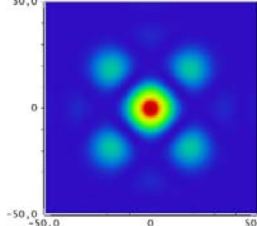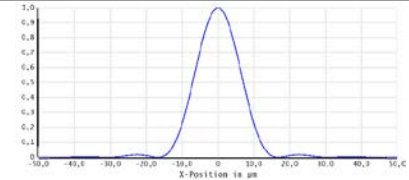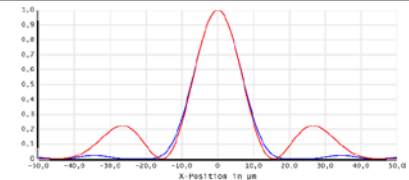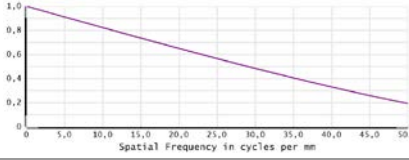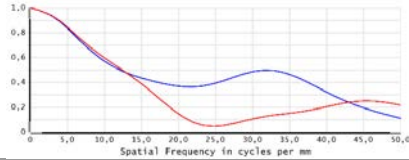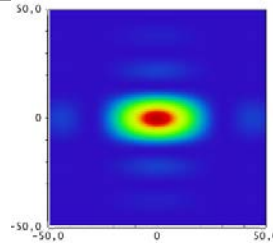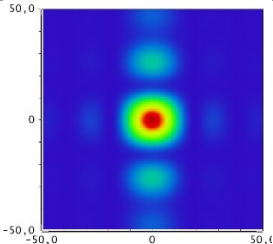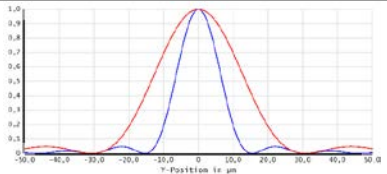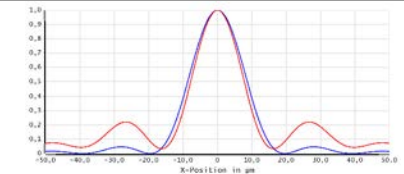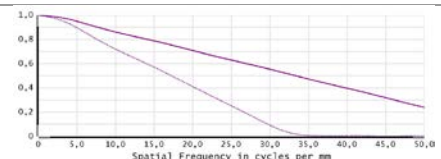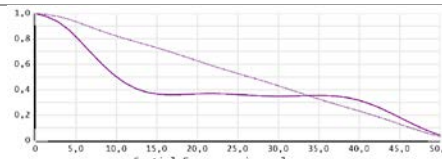
| | Circular | 4 Square |
|---|---|---|
| Size, shape of entrance pupil | 200mm diameter  | 100mm x 100mm (x 4)  |
| PSF |  |  |
| PSF cross-section x (and 45deg) |  |  |
| MTF curves X direction (and 45deg) |  |  |

**Table 3** One and two rectangular aperture based entrance pupils and their corresponding PSF-s.

| | Rectangular | 2 Rectangular |
|---|---|---|
| Size, shape of entrance pupil | 200mm x 100mm  | 200mm x 100mm + 200mm x 50mm  |
| PSF |  |  |
| PSF cross-section x and Y |  |  |
| MTF curves X and Y |  |  |

II. OPTICAL DESIGNS

*II. A. Non-freeform designs*

In this sections designs that use off-axis sections of rotationally symmetric surfaces are presented. The parent surfaces are rotationally symmetric polynomial aspheric surfaces, which are described by a polynomial expansion of the deviation from a conic surface. They already provide very good performance and we use these designs as starting points for the freeform optimization in the next section.

The definition of a freeform surface varies in literature, we consider a surface freeform when it lacks any rotational symmetry. Other definitions arise due to the complexity of the manufacturing procedures. Some of the surfaces in the present section are off-axis aspheres with large deviation from the best fit sphere (BFS) and they could be considered freeform (although the surface still has symmetry) because the complexity of the surface shape requires freeform manufacturing techniques. The surface would not be manufactured off-axis, but instead it would be centred during the ultraprecise fabrication process, e.g. using servo assisted diamond turning.

As it was mentioned in the previous section we will focus on the designs that are based on rectangular apertures, specifically, the ones illustrated in Table 3. Using requirements and design constrains outlined in Table 1, two optical designs were created; both based on a Three Mirror Anastigmat (TMA) using off-axis aspherical components. First, the layouts of the design with 200mm x 100mm rectangular entrance pupil (also the primary mirror) are depicted in Figure 1. The size of the deployable primary mirror equals the larger side of a 2U rectangular volume and the rest of the optical components are located inside the 2U volume. From the 3D layout it becomes apparent that there is plenty of space for e.g. non-optical components inside the 2U volume.

The Strehl ratio and the MTF curves of the design are shown in Figure 2. The image quality is very good, the design provides diffraction limited performance over the complete 1.1 x 1.1 degree$^2$ FOV (Strehl ratio > 0.8). The MTF on the other hand reveals that the contrast (and resolution) is not sufficient in the direction, which is perpendicular to the shorter side of the 200mm x 100mm aperture. Comparing the tangential and sagittal MTF curves, in tangential direction the MTF stays above 0.2 for the full field, but in sagittal direction the cut-off frequency is around 35 cycles per mm, which is lower than the Nyquist frequency.
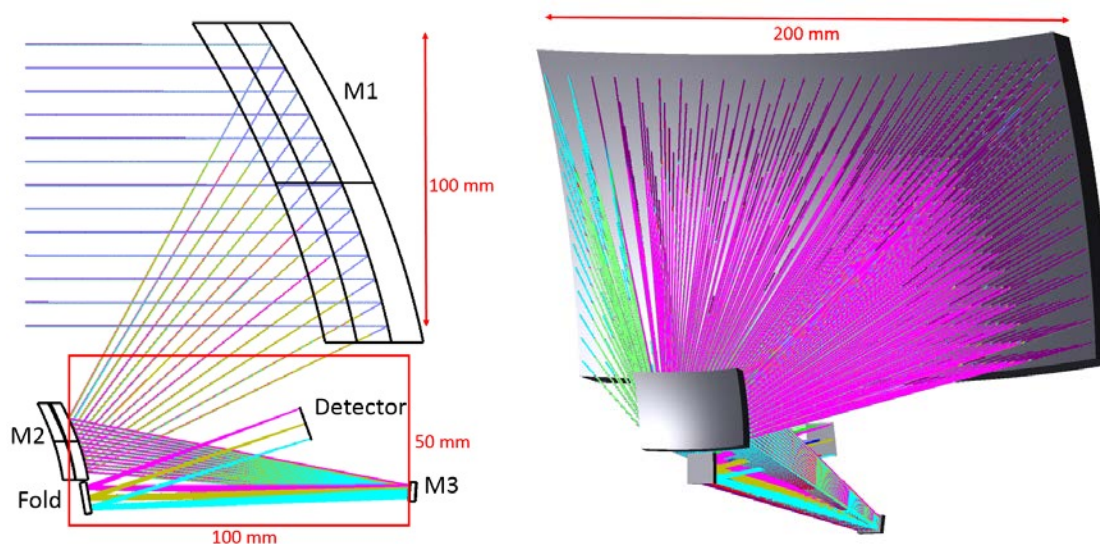


**Figure 1** The side view (left) and 3D view of the off-axis asphere based TMA with a 200mm x 100mm rectangular primary mirror. The 200mm x 100mm primary is deployable, the other mirrors are fixed.
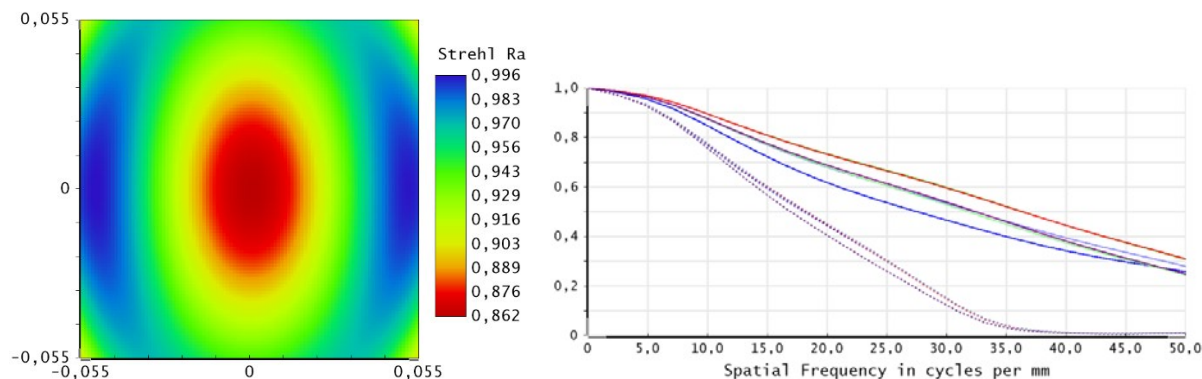
**Figure 2** On the left the RMS Strehl Ratio map of the design presented above is shown. The Strehl Ratio is better than 0.85 everywhere in the FOV, the worst being in the centre. In the right the PSF cross section in the centre of the FOV (worst case) is shown, FWHM is ~20 µm.

In the following a design based on two rectangular entrance pupils (also acting as primary mirror segments) is presented. The larger rectangular mirror is deployable and has a 200mm x 90mm size, the smaller primary mirror segment is fixed with the rest of the optical system, and it has a 200mm x 40mm size. All optical components are fixed and located in the 2U volume, except the deployable primary mirror. Two layouts of the design are shown in Figure 3 and the red 100mm x 100mm square corresponds to the cross section of the 2U volume. In order to have a completely unobscured optical system and avoid any vignetting, a very minor field offset is applied and also the primary mirror segments are smaller than what was prescribed in section I. M1-a and M1-b are the off-axis sections of the same parent optical axis and the concept is the same for M2-a and M2-b.

Although the entrance pupil area is increased with respect to the previous design, which ideally would improve the resolution and MTF performance in sagittal direction, due to large geometrical aberrations and reduced Strehl ratio, the resolution and MTF actually become worse. Some improvements can be achieved by tilting the focal plane surface and optimizing the surface shape of the fold mirror. Also, M1-a-and M2-a surfaces can be optimized independently from M1-b and M2-b to further improve image quality, but it still remains worse than the diffraction limit over a significantly large area of the field of view (the Strehl ratio map and the MTF curves for the design are shown in Figure 6).
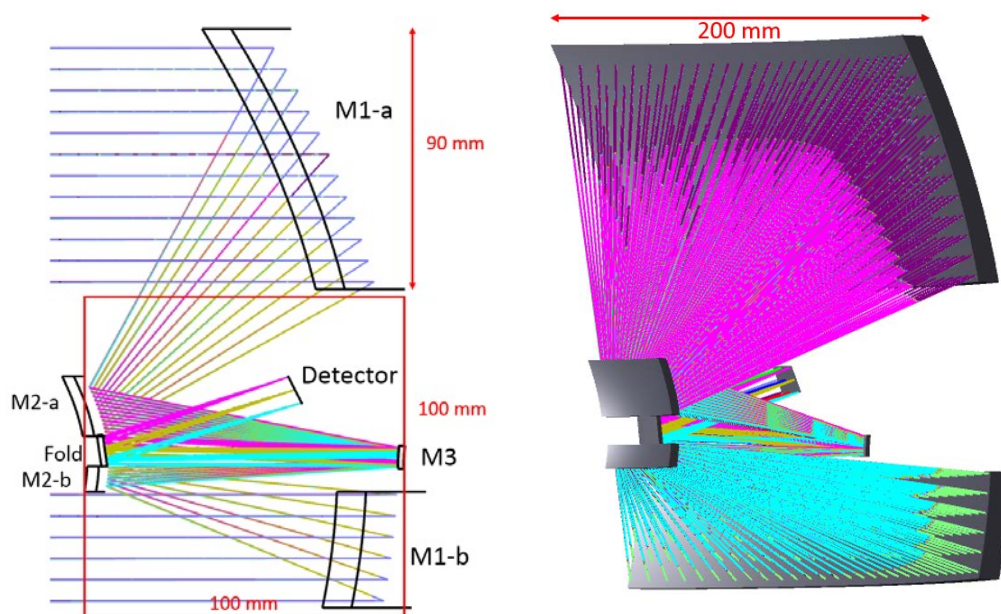


**Figure 3** The side view (left) and 3D view (right) of the off-axis asphere based TMA with two primary mirrors. One deployable with 200mm x 90mm size (M1-a) and one fixed with 200mm x 40mm size (M1-b). The red 100mm x 100mm box is the cross section of the 2U volume.

*II. B. Freeform designs*

The design shown in Figure 3 is the starting point for our freeform optimization. We set the following targets for the freeform optical system. On one hand, we would like to reduce the geometrical aberrations in the system and recover diffraction limited performance over the full FOV. Additionally, by tilting and decentering various optical components, we aim at creating a spatial arrangement, which improves mounting and packaging of the instrument and also decrease scattered light. We would like to investigate the possibility of further improving the MTF performance by increasing the size of the fixed primary segment. Finally, we investigate optical design that make use of square and TDI detectors as well, so we optimize using different FOV and focal plane shapes.

In Figure 4 and Figure 5 the layout of the first freeform based optical design is shown. By tilting M3, both M4 and the detector can be placed outside of the symmetry plane of the optical system (Figure 4, right). Having achieved that, both the size of M1-a (from 200mm x 90mm to 200mm x 100mm) and M1-b can be increased. In the case of the latter, a U-shaped aperture is created. The out of plane arrangement offers the possibility of placing baffles at various locations and thus achieves a more efficient scattered light reduction than before. In the optimization process, M2 and M4 were transformed into freeform surfaces, M1-a and M1-b still have the same parent optical surface, which is a rotationally symmetric asphere, M3 is a (centred) rotationally symmetric asphere.
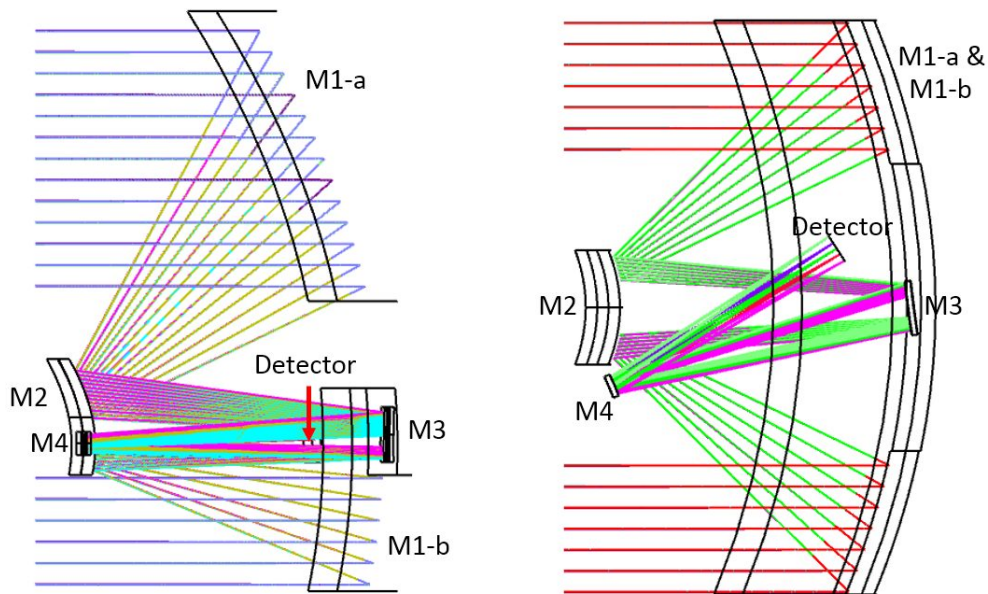


**Figure 4** The side view (left) and top view (right) is shown. By tilting M3, tilting/decentering M4 and at the same time optimizing with freeform surfaces, the image quality can be recovered.
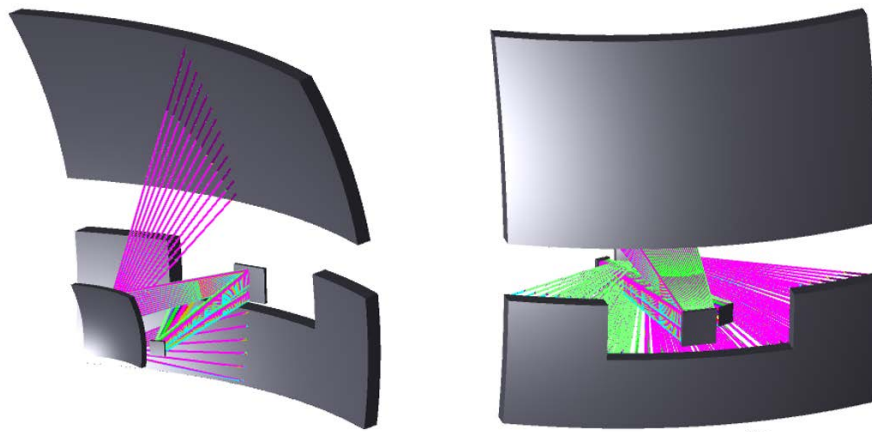


**Figure 5** 3D layouts of the design are shown. The two largest mirrors are the primary segments, the rectangular is a deployable and the U-shaped is fixed. By increasing the area of the primary mirror, the MTF can be improved significantly.

In the following the optical performance of the freeform design is compared to the rotationally symmetric design (Figure 3 in section II.A). The Strehl ratio and MTF curves are shown in Figure 6 for both designs and it becomes apparent that the freeform optical design improved significantly. It offers diffraction limited performance almost all over the square FOV and the MTF performance is also very good. The average MTF is higher than 0.2 at the Nyquist frequency higher and higher than 0.4 at the half of the Nyquist frequency. The design improved a lot with respect to the non-freeform optical design especially in contrast.
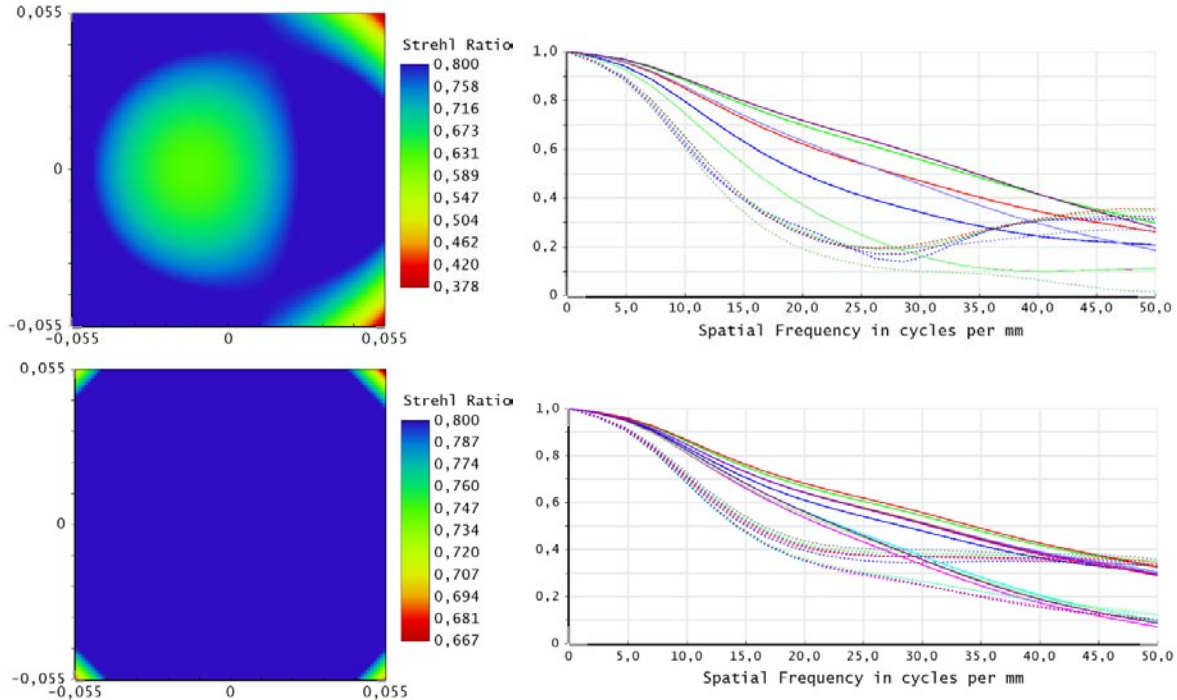


**Figure 6** The Strehl ratio (left) and the MTF curves (right) are shown for the non-freeform (top row) and freeform (bottom row) designs. The freeform optical design offers diffraction limited performance except the corners of the square FOV and the MTF performance is also very good, the average MTF is higher than 0.2 at the Nyquist frequency higher and higher than 0.4 at the half of the Nyquist frequency.

Another freeform based design is developed, which is based on a 2k x 128 stage TDI detector and thus have a very elongated focal plane area. In Figure 7 the 3D layout and the footprint on the freeform surface is shown. The M2 and M4 mirrors are merged into one freeform mirror, which is a monolithic mirror with multiple freeform surfaces. Similarly to the previous freeform based design, M1-a and M1-b have the same parent optical surface, which is a rotationally symmetric asphere and M3 is a (centred) rotationally symmetric asphere. The image quality is shown in Figure 8, it is diffraction limited over the full field of view and the MTF is also very promising.
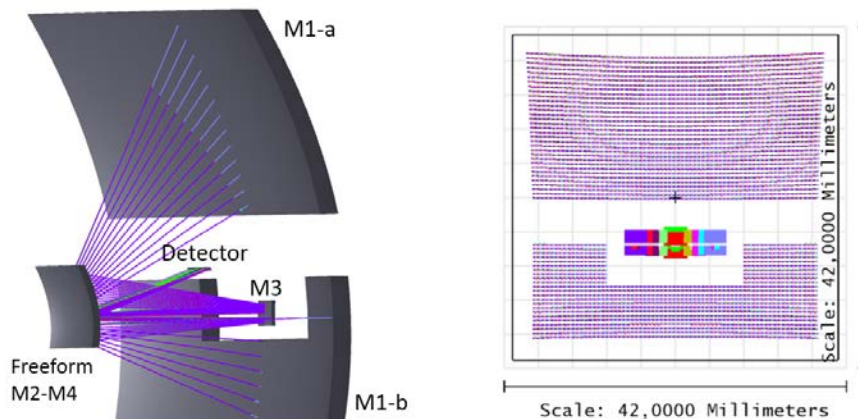


**Figure 7** A freeform based design with a 2k x 128 (stage) TDI detector is shown on the left. The freeform surface itself is the M2 and M4 in one surface. The footprint on the surface is shown on the right. M1-a is deployable, the other optical surfaces are fixed in the 2U volume.
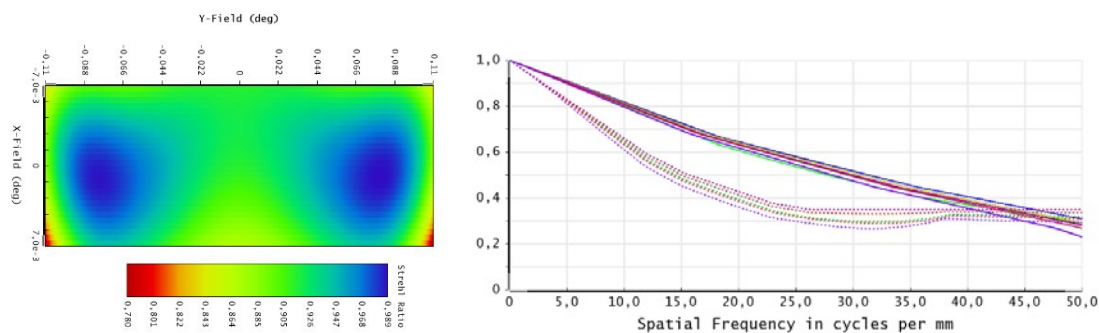
**Figure 8** The Strehl ratio and the MTF curves are shown for the freeform based optical design, which is based on the TDI detector.

*II. C. Freeform surface types and manufacturing*

We used two surface types that are both readily available in Zemax OpticStudio™, the optical design software that we were using during the freeform optical design optimization. The Zernike Standard Sag is defined by the same polynomial as the one that we used in the non-freeform optimization, plus additional aspheric terms defined by the Zernike Standard coefficients. The second surface type is described by a base radius of curvature and a sequence of Chebyshev polynomials, which is orthogonal over a rectangular area and so fits our purposes due to the rectangular mirror apertures in our designs. Still, most of the time, the Zernike Standard Sag surface type is proved to be more useful, probably because the starting point design is a TMA type optical system. Even, when the Chebyshev polynomials outperform the Zernike polynomials, a very high number of polynomial orders and coefficients are necessary to describe the surface, which makes the optimization process less efficient and global minima finding methods are needed to be implemented to avoid local minima in the optimization process. As usually in freeform optical design optimization, the careful selection of the field configuration, which essentially defines the input ray bundle is very important due to the necessity to achieve proper sampling on the freeform surface and homogeneous optical performance over the field.

There are several well established methods for freeform manufacturing. Small freeform lenses make use of developments in plastic/glass moulding technologies, components with larger sizes are realized by ultra precision milling, grinding and polishing. Diamond turning, a very common technique, can be successfully applied in many cases, but it has its limitations due to various factors, like temperature drifts, residual vibrations or undesired machining forces. If low surface form error (<500nm PV) and/or roughness (<3-5nm) is needed local figure correction techniques have to be used, e.g. ion beam figuring (IBF) or magnetorheological finishing (MRF). Applications, which require broad wavelength range utilize freeform mirrors, usually additional layers (electroless Ni) are applied to the substrate (Al, SiC) to increase local figure correction quality [2]. For the optical systems described in the present paper, the latter manufacturing methods would provide the performance that is necessary to achieve specifications.

III. CONCLUSIONS

We presented two freeform based optical designs that are suitable to be located in a CubeSat with 2U volume and are capable to deliver 1m resolution on the ground. One is based on a square detector format, the other is based on a TDI detector with 2k x 128 stage and they both offer diffraction limited performance at 550nm. Considering 10 µm pixel size, they are delivering an MTF of 0.2 at the Nyquist frequency and 0.4 at the half this frequency. Both of the designs have only one deployable primary mirror that has the size of 200mm x 100mm, covering the larger side of the 2U volume. There is another fixed primary segment that is located in the 2U volume together with the other optical components. Apart from the deployable primary mirror all the optical components are fixed. The deployable plus fixed primary mirror design offers various advantages in the alignment and integration phase and it also offers risk mitigation due to the fixed optical system that is capable to operate standalone. The optical design requires only one deployable mirror, less than required by other currently flying Earth observing satellites. Furthermore, the design is flexible and scalable, different sizes and focal ratios can be developed from the design presented in the paper.

ACKNOWLEDGMENTS

REFERENCES

[1] Hugot, E., et al., "Freeform active mirror experiment (FAME)," Proc. SPIE 9151, 9151-6 (2014).
[2] Beier, M., et al., "Development, fabrication, and testing of an anamorphic imaging snap-together freeform telescope," Appl. Opt. 54(12) 3530-3542 (2015).